Nondestructive thickness measurement of biological layers at the nanoscale by simultaneous topography and capacitance imaging

Ignacio Casuso, Laura Fumagalli, Gabriel Gomila, and Esteve Padrós

Citation: Applied Physics Letters **91**, 063111 (2007); doi: 10.1063/1.2767979
View online: http://dx.doi.org/10.1063/1.2767979
View Table of Contents: http://scitation.aip.org/content/aip/journal/apl/91/6?ver=pdfcov
Published by the AIP Publishing

Nondestructive thickness measurement of biological layers at the nanoscale by simultaneous topography and capacitance imaging

Ignacio Casuso,[a] Laura Fumagalli, and Gabriel Gomila
Departament d'Electrònica, Universitat de Barcelona and Laboratori de Nanobioenginyeria-IBEC, Parc Científic de Barcelona, Barcelona, Spain 08028

Esteve Padrós
Unitat de Biofísica, Department de Bioquímica i de Biologia Molecular, Facultat de Medicina i Centre d'Estudis en Biofísica, Universitat Autònoma de Barcelona, Barcelona, Spain 08193

(Received 30 May 2007; accepted 9 July 2007; published online 7 August 2007)

Nanoscale capacitance images of purple membrane layers are obtained simultaneously to topography in a nondestructive manner by operating alternating current sensing atomic force microscopy in jumping mode. Capacitance images show excellent agreement with theoretical modeling and prove to be a noninvasive method for measuring the thickness of purple membrane layers beyond the single monolayer limit with nanoscale lateral spatial resolution. With the ability of spatially resolving the capacitance while preserving the sample from damaging, this technique can be applied for nanoscale thickness measurement of other biological layers and soft materials in general. © *2007 American Institute of Physics*. [DOI: 10.1063/1.2767979]

Biological membranes and biomolecular self-assembled layers are being investigated as potential active materials in new micro- and nanoelectronic hybrid devices.[1–3] In its development, a main issue concerns the nondestructive measurement of the biolayer thickness with submonolayer thickness vertical resolution and submicrometric spatial lateral resolution. Standard thin film characterization techniques such as optical ellipsometry, reflectance spectroscopy,[4] and capacitance metrology[5,6] are not suitable for this purpose as they offer in all cases lateral resolution beyond the micrometer.

Recently, a new nanoscale capacitance metrology technique has been developed based on alternating current sensing atomic force microscopy (ac CS-AFM).[7–9] This technique has shown nanoscale spatial resolution in simultaneous capacitance and topographic imaging, thus enabling the evaluation of thin film thickness at the nanoscale.[10] However, until now, ac CS-AFM has been implemented in conventional AFM contact mode, which precludes its application to soft materials, such as biological layers, due to the large lateral shear forces inherent to this scanning mode.

In the present letter we describe the first implementation of ac CS-AFM in jumping mode (JM),[11,12] and show its use as a nondestructive technique for nanoscale capacitance imaging and thickness characterisation of biological layers and soft materials, in general, that enables individual capacitance characterization at fix points of the sample in control of the applied force and time of measurement in addition to minimal shear forces during lateral motion.

The experimental setup developed consists of a commercial AFM (Nanotec Electronica S.L.) connected to a fully customized amplifier,[13] which allows simultaneous topographic and low-noise dc and ac current measurements. Images are produced by jumping a conductive tip biased with respect to the sample at each image point following the sequence: tip retraction, lateral displacement, and approach down to contact, as schematically shown in Fig. 1, and described elsewhere.[11] In this way, the probe produces minimum lateral shear forces on the samples during the scan while allowing for simultaneous contact electrical measurements. The electric current flowing through the tip is acquired at each image point by the WSXM software[14] during the period of the cycle when the tip is in contact with the sample surface, together with the conventional AFM signals, thus producing four simultaneous images: topography, dc current, ac resistance, and capacitance. With respect to dc current measurements, ac current measurements are much more technically demanding as one has to measure extremely small capacitance variations (attofarad range) in the presence of a large stray contribution (~100 fF range).[7] In order to reach this capacitance sensitivity we either set long acquisition times per point or average out several consecutive measurements taken on the same line scan.

As a model system of biological layer, we used purple membrane (PM) layers, a two-dimensional crystal lattice naturally present in the cell membrane of *Halobacterium Salinarum*.[15] PM is composed of a lipid bilayer and a single protein species, the *Bacteriorhodopsin* (bR), in a lipid-to-protein ratio of 10 (mol/mol). PM shows functional response in both dry and humid conditions (following different

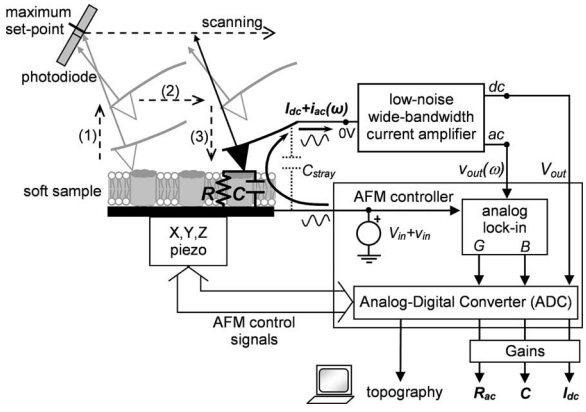

FIG. 1. Schematic representation of the setup used for current-sensing AFM (CS-AFM) in jumping mode (JM). Simultaneous images of topography, dc current I_{dc}, ac resistance R_{ac}, and capacitance C can be obtained with almost no lateral shear forces.

[a]Electronic mail: icasuso@pcb.ub.es

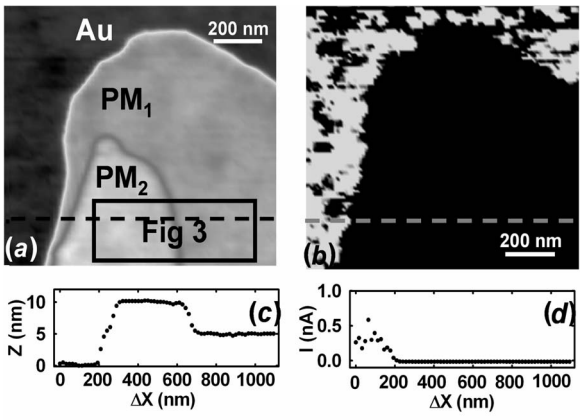

FIG. 2. Simultaneous topographic (a) and dc current (b) images of a PM patch on a gold substrate measured by dc CS-AFM in jumping mode with 100 mV applied bias. Profiles of (c) topography and (d) direct current corresponding to the dashed lines in the images are also shown. The PM patch is formed by an ~5 nm thick monolayer (PM_1) which is double folded in some regions (PM_2).

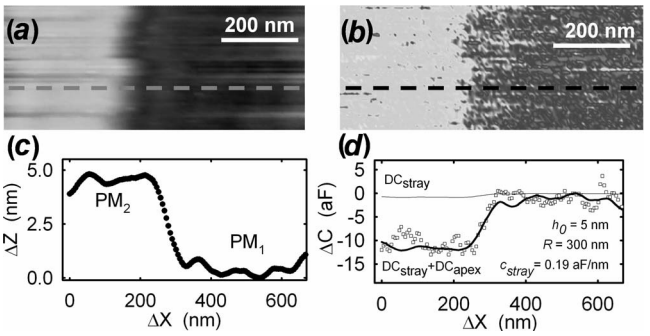

FIG. 3. Simultaneous (a) topographic and (b) capacitance images of a PM membrane step [marked area in Fig. 2(a)] measured by ac CS-AFM in jumping mode. Profiles of (c) topography and (d) capacitance (squares) corresponding to the dashed line in the images are also shown. The theoretical capacitance profile calculated with a PM_1 thickness of h_0=5 nm is shown in (d) (solid thick line), showing excellent agreement with observed data. The stray capacitance contribution (solid thin line) is shown to be negligible.

photocycles) and has been proposed as an excellent candidate for hybrid bioelectronic devices.[16–18]

Patches of PM containing wild type bR were deposited onto a flat gold film evaporated on a mica substrate and dried under N_2(g) flow. To avoid large current values, a resistor of 120 MΩ was added in series with the sample. All the measurements were performed under dry N_2(g) conditions and using conductive diamond coated tips (CDT force modulation mode Nanosensors™, nominal radius of 100–200 nm and spring constant of 2.8 N/m).

We first obtained simultaneous topographic and dc current images in jumping mode of the PM patches in order to verify its insulating and homogeneous nature. Figure 2 shows characteristic images obtained by applying a 3 nN force and a dc bias of 100 mV.

The topographic image [Fig. 2(a)] reveals a PM patch formed by an ~5 nm thick monolayer (PM_1) which is double folded in some regions (PM_2). The corresponding dc current image [Fig. 2(b)] shows current levels through the PM patch (dark region) below the amplifier resolution (~0.3 pA), surrounded by a highly conductive region corresponding to the gold substrate with current levels up to 0.8 nA (here the current level is limited by the series resistor). The irregular conductivity of the gold is due to the contamination residues from the PM solution, which impedes a good electrical contact with the gold substrate in some regions. The PM patch shows a low voltage uniform insulating nature, compatible with a pure capacitive behavior. During several hours of JM scanning no appreciably deformation of the biological layer was observed, thus proving the ability of jumping mode to perform simultaneous topographic and electric measurements without destroying or appreciably deforming the biological layer.

Simultaneous topographic and capacitance images obtained on a small portion of the PM patch shown in Fig. 2(a) are shown in Fig. 3. Measurements have been taken at the same applied force (3 nN), with an applied sinusoidal voltage of 0.7 V_{rms} amplitude and 92 kHz frequency, and 0 V dc bias. The images have been taken at low scan rate (143 ms/pixel) to reach high capacitance resolution [below 3 aF in Fig. 3(b)]. Figure 3 clearly shows a direct correlation between membrane topography and capacitance, thus showing the ability of ac CS-AFM in jumping mode to image both properties simultaneously. This correlation between topography and capacitance is further evidenced through the profiles taken along one scanning line [Figs. 3(c) and 3(d)], in which a capacitance variations of a few attofarads precisely tracks the topography profile of the monolayer PM_2 over the first layer PM_1. The integrity of the PM membrane patch has remained unaffected again during the imaging process. Importantly, we remark that before Fig. 3 no other nanoscale capacitance image on a biological specimen had ever been reported.

Higher capacitance sensitivity (around 1 aF) can be obtained by averaging out a number of consecutive scans taken on the same line. An example is shown in Fig. 4. We note that further slowing down the scan speed to increase capacitance sensitivity is subject to scan instabilities. The profiles shown in Figs. 4(c) and 4(d) have been obtained by averaging out nine consecutive scans taken at a scan speed of 56 ms/pixel on a PM patch showing three overlapping layers [Fig 4(a)] and using a different AFM probe. We found that the averaged topographic and capacitance profiles [Figs. 4(c) and 4(d)] show again an excellent correlation, but this time with lower capacitance noise.

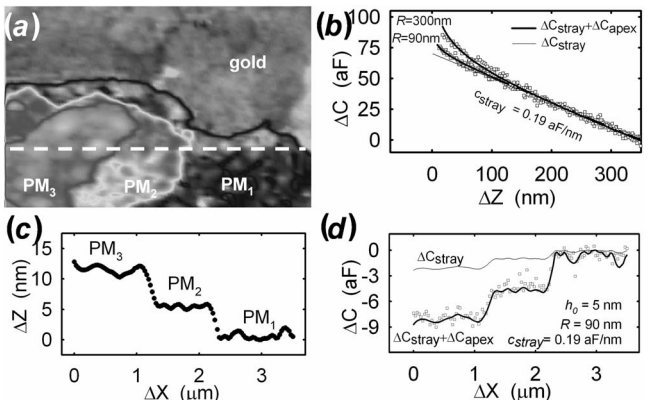

FIG. 4. (a) Topographic image of three partially overlapping PM monolayers. (b) Capacitance distance curve taken on the gold surface close to the PM patch (symbols) used to calibrate the stray capacitance (thin solid line) and the effective electrical radius of the tip apex (thick solid line). Averaged (c) topographic and (d) capacitance profiles taken along the dashed line in (a). In (d) symbols represent the measurements, the solid line the theoretical expectation for a thickness h_0=5 nm of PM_1 and the thin solid line the stray capacitance contribution (below 2 aF).

The results reported in Figs. 3 and 4 can be interpreted in a quantitative way and hence used to accurately determine the membrane thickness with nanoscale lateral and vertical spatial resolutions. We remark that while here the reference thickness h_0 could be also obtained from the larger area topographic image in general this will not be the case. The technique reported here will then constitute a powerful and nondestructive method to assess the thickness of the biolayers. To this aim, a theoretical model of the tip/membrane/gold substrate capacitance as a function of layer thickness under dry conditions is necessary. This model can be obtained from a recent derivation of the electrostatic force acting on a conductive tip in close proximity to a thin dielectric film,[19]

$$F_{\text{apex}}(z,h) = -\pi\varepsilon_0 V^2 \frac{R}{z + h/\varepsilon}, \tag{1}$$

where h is the layer thickness, ε its dielectric constant, z the tip-thin film distance, and V the tip-electrode substrate voltage. The tip capacitance as a function of tip-membrane distance and membrane thickness is then given by

$$C_{\text{apex}}(z,h) \equiv \int \frac{2F(z,h)}{V^2} dz + K(R)$$
$$= -2\pi\varepsilon_0 R \ln\left(\frac{R}{z + h/\varepsilon}\right) + K(R), \tag{2}$$

where $K(R)$ is a constant value depending on the tip radius. The capacitance variation as a function of a change in membrane thickness Δh with respect to a given thickness of reference h_0 can then be evaluated as

$$\Delta C_{\text{apex}}(\Delta h, h_0) \equiv C_{\text{apex}}(0, h_0 + \Delta h) - C_{\text{apex}}(0, h_0)$$
$$\equiv -2\pi\varepsilon_0 R \ln\left(\frac{h_0 + \Delta h}{h_0}\right), \tag{3}$$

Equation (3) holds true provided that the dielectric constant of the layer is homogeneous and that $\varepsilon R \gg h_0$, $h_0 + \Delta h$, as in the present case. Note that within this approximation the local capacitance due to a change in thickness is independent from the dielectric constant and only depends on the sample thickness. The measured capacitance in an ac CS-AFM experiment includes in addition a contribution from the stray capacitance variation that can be approximated by a linear function of the profile changes,[7] thus giving

$$\Delta C_{\text{meas}}(\Delta h, h_0) \equiv \Delta C_{\text{stray}}(\Delta h, h_0) + \Delta C_{\text{apex}}(\Delta h, h_0)$$
$$\equiv -c_{\text{stray}} \Delta h - 2\pi\varepsilon_0 R \ln\left(\frac{h_0 + \Delta h}{h_0}\right), \tag{4}$$

Equation (4) can be used to interpret quantitatively the capacitance measurements and to extract from them the biolayer thickness. To this end, we first determine the stray capacitance rate c_{stray} and the tip radius R from the capacitance-distance curves on bare gold shown in Fig. 4(b) as reported elsewhere.[7] For the two tips used in the experiments we obtain $c_{\text{stray}} = 0.19 \pm 0.05$ aF/nm, $R_{\text{Fig. 3}} = 300 \pm 30$ nm, and $R_{\text{Fig. 4}} = 90 \pm 9$ nm. Then, we obtain the thickness variation Δh from the simultaneously measured topographic profile [Figs. 3(c) and 4(c)]. Finally, we fit the measured capacitance to Eq. (4) by adjusting the only remaining free parameter, the thickness of the first PM layer (PM_1), h_0.

We obtain $h_0 = 5.0 \pm 0.8$ nm and $h_0 = 5 \pm 1$ nm in both cases from data in Figs. 3(d) and 4(d). The agreement between theoretical and experimental data is excellent in both cases. The obtained thickness of the reference layer (5 nm) perfectly fits the thickness of the bottom PM monolayer (PM_1) measured from the larger area topographic image [Figs. 2(a) and 4(a)]. In addition, the extracted value of the membrane thickness proves to be independent from the electrical tip radius of the measuring probe. These results then demonstrate the ability of simultaneous topographic and capacitance measurements to provide membrane layer thickness values at the nanoscale.

In summary, we have demonstrated the ability of ac current-sensing AFM operated in jumping mode to map simultaneously the topography and capacitance of biological layers without damaging them. We have shown that by means of these measurements the biolayer thickness can be determined with high precision at the nanoscale. With the ability of spatially resolving the capacitance while preserving the sample from damaging, this technique can be applied for nanoscale thickness measurement of other biological layers and soft materials in general

Financial support by BFU2006-04656/BMC and NAN2004-09415-C05-01 grants of the Spanish MEC is acknowledged. The authors are grateful to M. Sampietro and G. Ferrari (Politecnico di Milano) for the electronic circuitry and to Nanotec Electronica S.L. for assistance in the AFM setup.

[1] J. J. Davis, D. A. Morgan, C. L. Wrathmell, D. N. Axford, J. Zhao, and N. Wang, J. Mater. Chem. **15**, 2160 (2005).
[2] K. J. Wise, N. B. Gillespie, J. A. Stuart, M. P. Krebs, and R. R. Birge, Trends Biotechnol. **20**, 387 (2002).
[3] G. Gomila, I. Casuso, A. Errachid, O. Ruiz, E. Pajot, J. Minic, T. Gorojankina, M. A. Persuy, J. Aioun, R. Salesse, J. Bausells, G. Villanueva, G. Rius, Y. Hou, N. Jaffrezic, C. Pennetta, E. Alfinito, V. Akimov, L. Reggiani, G. Ferrari, L. Fumagalli, M. Sampietro, and J. Samitier, Sens. Actuators B **116**, 66 (2006).
[4] H. G. Tompkins and W. A. McGahan, *Spectroscopic Ellipsometry and Reflectometry: A User's Guide* (Wiley, New York, 1998), p. 36.
[5] J. Graham, M. Kryzeminski, and Z. Popovic, Rev. Sci. Instrum. **71**, 2219 (2000).
[6] A. Guadarrama-Santana and A. Garcia-Valenzuela, IEEE Trans. Instrum. Meas. **56**, 107 (2007).
[7] L. Fumagalli, G. Ferrari, M. Sampietro, I. Casuso, E. Martinez, J. Samitier, and G. Gomila, Nanotechnology **17**, 4581 (2006).
[8] D. T. Lee, J. P. Pelz, and B. Bhushan, Rev. Sci. Instrum. **73**, 3525 (2002).
[9] F. Houzé, P. Chretien, O. Schneegans, R. Meyer, and L. Boyer, Appl. Phys. Lett. **86**, 123103 (2005).
[10] D. T. Lee, J. P. Pelz, and B. Bhushan, Nanotechnology **17**, 1484 (2006).
[11] P. J. de Pablo, J. Colchero, J. Gomez-Herrero, and A. M. Baro, Appl. Phys. Lett. **73**, 3300 (1998).
[12] C. Gómez-Navarro, P. J. de Pablo, J. Colchero, Y. Fan, M. Burghard, J. Gomez-Herrero, and A. M. Baro, Nanotechnology **14**, 134 (2003).
[13] M. Sampietro, G. Ferrari, and D. Natali, International Patent No. WO 2005/062061 (July 7, 2005).
[14] I. Horcas, R. Fernandez, J. M. Gomez-Rodriguez, J. Colchero, J. Gomez-Herrero, and A. M. Baro, Rev. Sci. Instrum. **78**, 013705 (2007).
[15] D. Oesterhelt and W. Stoeckenius, Proc. Natl. Acad. Sci. U.S.A. **70**, 2853 (1973).
[16] J. Shin, P. Bhattacharya, J. Xu, and G. Varo, Opt. Lett. **29**, 2264 (2004).
[17] W. W. Wang, G. K. Knopf, and A. S. Bassi, Biosens. Bioelectron. **21** 1309 (2006).
[18] J. Shin, P. Bhattacharya, Y. Hao-Chih, and M. Zhenqiang, Opt. Lett. **32**, 500 (2007).
[19] G. M. Sacha, E. Sahagun, and J. J. Sáenz, J. Appl. Phys. **101**, 024310 (2007).